Journal of Hazardous Materials 170 (2009) 1197–1203

Contents lists available at ScienceDirect

Journal of Hazardous Materials

journal homepage: www.elsevier.com/locate/jhazmat

Sorption behavior of nano-TiO_2 for the removal of selenium ions from aqueous solution

Lei Zhang*, Na Liu, Lijun Yang, Qing Lin

College of Chemistry, Liaoning University, 66 Chongshan Middle Road, Shenyang 110036, People's Republic of China

ARTICLE INFO

Article history:
Received 26 December 2008
Received in revised form 19 May 2009
Accepted 20 May 2009
Available online 27 May 2009

Keywords:
Selenium
Nano-TiO_2
Removal
Kinetics
Thermodynamics

ABSTRACT

Titanium dioxide nanoparticles were employed for the sorption of selenium ions from aqueous solution. The process was studied in detail by varying the sorption time, pH, and temperature. The sorption was found to be fast, and to reach equilibrium basically within 5.0 min. The sorption has been optimized with respect to the pH, maximum sorption has been achieved from solution of pH 2–6. Sorbed Se(IV) and Se(VI) were desorbed with 2.0 mL 0.1 mol L^{-1} NaOH. The kinetics and thermodynamics of the sorption of Se(IV) onto Nano-TiO_2 have been studied. The kinetic experimental data properly correlate with the second-order kinetic model (k_2 = 0.69 g mg^{-1} min^{-1}, 293 K). The overall rate process appears to be influenced by both boundary layer diffusion and intraparticle diffusion. The sorption data could be well interpreted by the Langmuir sorption isotherm. The mean energy of adsorption (14.46 kJ mol^{-1}) was calculated from the Dubinin–Radushkevich (D–R) adsorption isotherm at room temperature. The thermodynamic parameters for the sorption were also determined, and the ΔH^0 and ΔG^0 values indicate exothermic behavior.

1. Introduction

Selenium is an important micronutrient for human and animal health, but at elevated concentrations selenium toxicity is a concern [1]. The removal of selenium from water has an increasing concern because of their involvement in many industries. Selenium is found in the effluents in the form of selenate (SeO_4^{2-}) and selenite (SeO_3^{2-}) from thermal power stations, oil refineries and smelting plants in addition to the industries of glass production, pigments, solar batteries and semiconductors [2]. Therefore, a convenient and simple method with a high adsorption capacity is necessary for removing different oxidation states of selenium present in the environment.

Physicochemical methods such as chemical precipitation, catalytic reduction and ion exchange have been mainly used for the removal of soluble selenium, however, they are costly [3]. Sorption studies have been utilized to understand the mobility and bioavailability of selenium in diverse systems, e.g. aluminium oxide [4], manganese nodules [5], haematite [6], activated carbon [7], modified rice husk [8], peanut shell [9] and magnetite [10].

Nanoparticles have high adsorption capacity. Besides, the operation is simple, and the adsorption process rapid. In this paper, nano-TiO_2 sorbent was used to remove selenium from aqueous solutions for the first time. The study was carried out with the aim to optimize conditions for maximum removal of selenium ions from aqueous solutions on nano-TiO_2 surface in the absence and presence of various ions. Besides this, the adsorption data was fitted to various equations to obtain constants related to the equilibrium and kinetics of the adsorption phenomena.

2. Experimental

2.1. Apparatus

UV-Vis-NIR Cary 5000 (VARIAN Co., US) was used to measure the concentration of selenium. A S-3C Model pH meter (Shanghai Precision Scientific Instrument Co., China) was used for measuring the pH of solutions. A model KQ-100B ultrasonic cleaner (Kunshan Ultrasonic Instrument Co., China) and a model TDL80-2B centrifugal machine (Shanghai Anting Scientific Instrument Co., China) were used throughout. The nano-TiO_2 powders X-ray diffraction (XRD) patterns were recorded on Siemens D5000 Diffractometer. The morphology of TiO_2 particles was determined by transmission electron microscopy (TEM, Hitachi 800).

2.2. Reagents

All the other reagents including Arabic gum solution (10%), Malachite green solution (0.05%), potassium iodide (10%), hydrochloric acid, nitric acid and sodium hydroxide, were of analytical grade and obtained from Shanghai Xinzhong Chemical Reagent Co., China. Doubly distilled water was used throughout experiments.

* Corresponding author. Tel.: +86 24 62202380; fax: +86 24 62202380.
E-mail address: zhanglei63@126.com (L. Zhang).

0304-3894/$ – see front matter © 2009 Published by Elsevier B.V.
doi:10.1016/j.jhazmat.2009.05.098

Nano-TiO_2 (anatase) that was used as sorbent in this study was provided from Zhoushanmingri Nanometer Material Co., China and its particle size was about 10–15 nm.

The preparation of a stock solution of Se(IV) (1.000 mg mL^{-1}): 1.0000 g of Se (Beijing Xingta Chemical Co., China) was added into 50 mL (1 + 1) HNO_3 solution, and heating in boiling water bath to dissolve it, then added 5 mL sulfuric acid. The solution was heated continuously until the solution become transparent, finally diluted to a 1 L volumetric flask with doubly distilled water [11].

A 1.000 mg mL^{-1} Se(VI) standard stock solution was prepared by dissolving 0.2393 g Na_2SeO_4 in water and diluting to the mark in a 100 mL volumetric flask.

2.3. Procedure

2.3.1. Determination of Se(IV)

Some volumes of Se(IV) standard solution were put into 25 mL volumetric flasks, then 1.0 mL 6.0 mol L^{-1} HCl, 3.0 mL 0.05% Malachite green, 3.0 mL 10% KI and 3.0 mL 10% Arabic gum solution were added into the volumetric flasks. Double-distilled water was put into the solutions to prepare desired volumes and shaken up. After 30 min, absorbency was determined by UV–vis spectrometer at wavelength of 670 nm with 1 cm quartz cell, and the content of the Se(IV) was obtained.

2.3.2. Determination of Se(VI)

Some of Se(VI) standard solution were transferred into a 10 mL tube, adding the same volume of 9 mol L^{-1} hydrochloric acid, heating it with boiling water bath some time, cooling it, Se(VI) has been reduced to Se(IV). A portion of the solution was measured according to Section 2.3.1.

2.3.3. Adsorption of selenium on nano-TiO_2

The sorption experiments were carried out in a series of 50 mL Erlenmeyer flasks containing 0.05 g nano-TiO_2 and 10.0 mL of 20.0 mg L^{-1} selenium solution at pH 5. If necessary, an appropriate volume of HCl or NaOH solutions was used to adjust the pH of the solution before the addition of nano-TiO_2. After ultrasonic dispersion for 3 min and static adsorption for 10 min, the two phases were separated by centrifuging at 4000 rpm for 5 min. The concentration of selenium ions was determined by UV-Vis-NIR Cary 5000. The sorption percentage (*Ads.%*) was calculated as:

$$Ads.\% = \frac{C_0 - C_e}{C_0} \times 100 \quad (1)$$

where C_0 and C_e are the initial and the final concentration of selenium in solution phase, respectively.

Adsorption isotherm studies were carried out with different initial concentrations of selenium while maintaining the sorbent dosage at constant level. In order to inspect any adsorption of selenium on the container surface, control experiments were carried out without the sorbent. It was found that no adsorption occurred on the container wall.

Kinetic experiments were conducted using a known weight of the sorbent dosage in the range of 273–313 K. After regular intervals of time, suitable aliquots were analyzed for selenium concentration. The rate constants were calculated using the conventional rate expression.

The thermodynamic parameters for the process of adsorption were determined at a particular temperature. This procedure was repeated at three different temperatures ranging from 273 K to 313 K.

Table 1
Effect of different sorbents on adsorption behavior.

Sorbents	*Ads.%*
Nano-TiO_2 (anatase 10–15 nm)	96.8
Nano-TiO_2 (rutile 10–15 nm)	93.0
Nano-Al_2O_3 (γ, 10 nm)	79.3
Nano-SiO_2 (20 nm)	0.1

Data indicate that model parameters are statistically significant (*t*-test) at 95% confidence level.

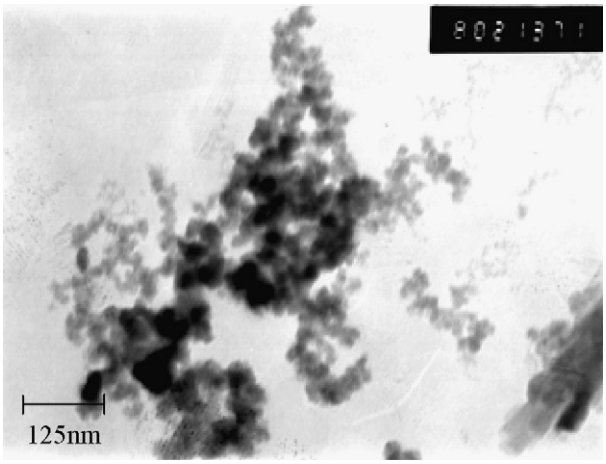

Fig. 1. TEM micrographs of nano-TiO_2 powders.

3. Results and discussion

3.1. Selection of sorbent

The effect of different sorbents on the adsorption behavior for selenium in aqueous solution was studied and shown in Table 1. It was found that the nano-TiO_2 (anatase) was the best sorbent.

3.2. Characterization of nanometer TiO_2

The TEM image of nano-TiO_2 is shown in Fig. 1. The TEM image shows dense microstructure and granular grain. The average grain size of nano-TiO_2 is about 10–15 nm.

The crystal structure of nano-TiO_2 was characterized using XRD for 2θ diffraction angles from 20° to 80° was shown in Fig. 2. The sharp peaks at 25.29°, 37.78° and 48.20° can be attributed to anatase

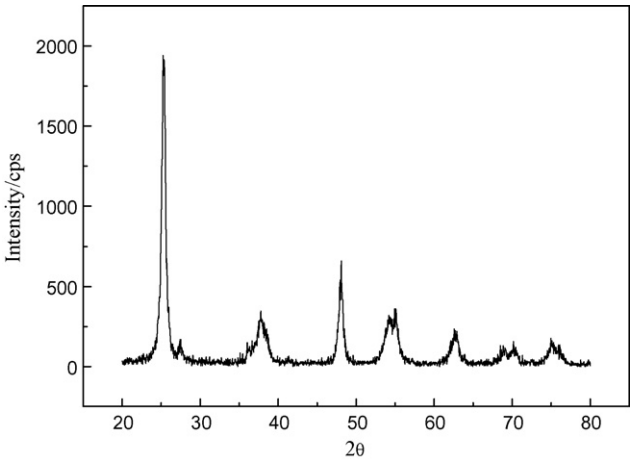

Fig. 2. XRD pattern of nano-TiO_2 powders.

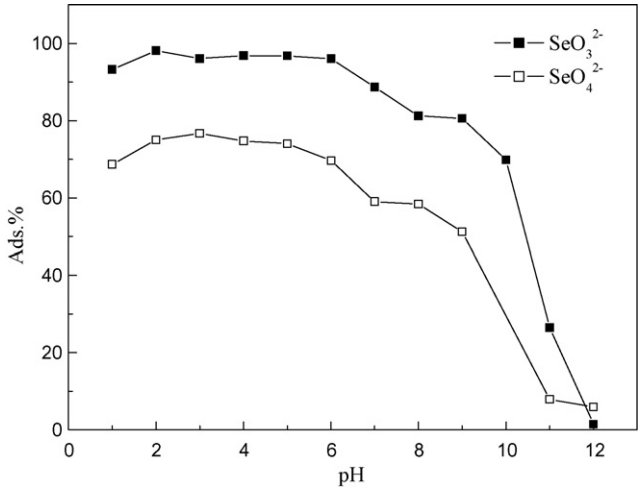

Fig. 3. Effect of pH on the adsorption efficiency of Se(IV) and Se(VI) on nano-TiO_2; 50 mg nano-TiO_2; $C_{Se(IV)}$: 20.0 mg L^{-1}, $C_{Se(VI)}$: 20.0 mg L^{-1}; temperature 20 ± 0.1 °C.

TiO_2 according to the standard pattern of anatase TiO_2. It can be concluded that nano-TiO_2 existed as anatase structure.

3.3. Effect of pH

We applied 10 mL of 20.0 mg L^{-1} of Se(IV) or Se(VI) to test the sorption of selenium onto nano-TiO_2 at different pH values. The results show (Fig. 3) that both selenite and selenate species adsorb onto nano-TiO_2, but the affinity for Se(VI) is generally smaller than for Se(IV). A removal percentage (>96%) was found for Se(IV) in the pH range of 2–6, and for Se(VI), only about 76% was removed from the testing solution. As the solution pH increases (pH > 6) Se(IV) and Se(VI) sorption decreases, with the lowest uptake occurring at pH 12.

This phenomenon is consistent to the pK_a values of selenious and selenic acids. Se(IV) species in aqueous solution include selenious acid (H_2SeO_3), biselenite ($HSeO_3^-$) and selenite (SeO_3^{2-}). Between pH 3.5 and 9.0, biselenite is the predominant ion in water. Above pH 9.0 selenite species dominates and as pH decreases below pH 3.5 [12], selenious acid dominates. The pK_a of selenic acid is 1.92, selenate (SeO_4^{2-}) is the dominant species when pH > 1.9 [13]. Therefore, biselenite ($HSeO_3^-$) and selenate (SeO_4^{2-}) was the dominant species when pH ranges from 2 to 6, selenite (SeO_3^{2-}) and selenate (SeO_4^{2-}) are predominant ions in the alkaline medium.

The surface charge of the nano-TiO_2 is neutral at isoelectric point (IEP) [14], which pH_{IEP} value is 6.8 for nano-TiO_2. The surface of sorbent carries positive charges at pH value lower than IEP, which enhances electrostatic force of attraction with biselenite and selenate ions. At higher pH_{IEP}, there exists electrostatic repulsion between the negative charged of the sorbent, selenite and selenate anions would result in a release of the adsorbed selenium. Therefore, the highest adsorption was obtained in the pH range of 2–6, pH 5 was chosen for the sorption of selenium ions in the experiment.

3.4. Desorption studies

It is found from Fig. 3 that the adsorption of anions at pH > 12 could be negligible. For this reason, the solutions of various concentration NaOH were studied for the elution of retained selenium ions from nano-TiO_2. The effect of eluent volume on the desorption of analytes was also studied at the optimum concentration of the eluent (2.0 mL, 0.1 mol L^{-1} NaOH), it was found that with 2.0 mL 0.1 mol L^{-1} NaOH elution percentage (>95%) could be obtained within 5 min. Therefore, the volume of 2.0 mL 0.1 mol L^{-1} NaOH was used to desorb selenium ions.

3.5. Adsorption kinetic model

Se(IV) and Se(VI) are the most common inorganic forms of selenium. For humans and most other mammals, selenite (SeO_3^{2-}) are more toxic than selenate (SeO_4^{2-}). Hence, adsorption behavior of Se(IV) was primarily investigated in this paper.

The kinetics of the sorption of Se(IV) onto-TiO_2 was investigated by agitating 10 mL of solution containing 30.0 mg L^{-1} Se(IV), pH 5 with 50 mg of onto-TiO_2 in the range of 0–5.0 min. The sorption percentage was obtained by determining the amount of selenium remained in the solution. In this experiment, it was verified that the sorption equilibrium was attained near to 5.0 min. It is well recognized that the characteristic of sorbent surface is a critical factor that affect the sorption rate parameters and that film resistance plays an important role in the overall transport of the solute. In order to quantify the changes in the sorption of Se(IV) with time, an appropriate kinetic model would be required. Therefore the different kinetic models were tested.

The sorption kinetics may be described by the pseudo-first-order Lagergren rate model. The equation is as follows [15]:

$$\lg(q_1 - q_t) = \lg\ q_1 - \frac{k_1 t}{2.303} \quad (2)$$

where q_1 and q_t are the amounts of Se(IV) adsorbed on the sorbent (mg g^{-1}) at equilibrium and at time t, respectively, and k_1 is the rate constant of the first-order adsorption (min^{-1}). The straight-line plots of $\lg(q_1 - q_t)$ against t were used to determine the rate constant, k_1 and correlation coefficient, r_1 values of the Se(IV) under different concentration range were calculated from these plots.

A pseudo-second-order [15] model may also describe the kinetics of sorption of selenium on nano-TiO_2, the equation may be expressed as follows:

$$\frac{t}{q_t} = \frac{1}{k_2 q_2^2} + \frac{t}{q_2} \quad (3)$$

where k_2 is the rate constant of the second-order adsorption (g mg^{-1} min^{-1}). The straight-line plots of t/q_t against t have been tested to obtain rate parameters.

The batch kinetic data were fitted to both the above models. Both models adequately described the kinetic data at 95% confidence level. The results of the kinetic parameters for Se(IV) adsorption are listed in Table 2. Based on the correlation coefficients, the adsorption of Se(IV) is best described by the pseudo-second-order equation.

It was possible to calculate the activation energy for adsorption employing Arrhenius equation for the rate constant based on the

Table 2
Kinetic parameters for Se(IV) adsorption on nano-TiO_2 at the different temperatures.

T (K)	k_1 (min^{-1})	q_1 (mg g^{-1})	r_1	k_2 (g mg^{-1} min^{-1})	q_2 (mg g^{-1})	r_2
273	0.67	5.61	0.992	0.33	6.00	0.999
293	0.54	5.36	0.965	0.69	5.46	0.999
313	0.77	5.07	0.992	1.12	5.20	0.999

Data indicate that model parameters are statistically significant (t-test) at 95% confidence level.

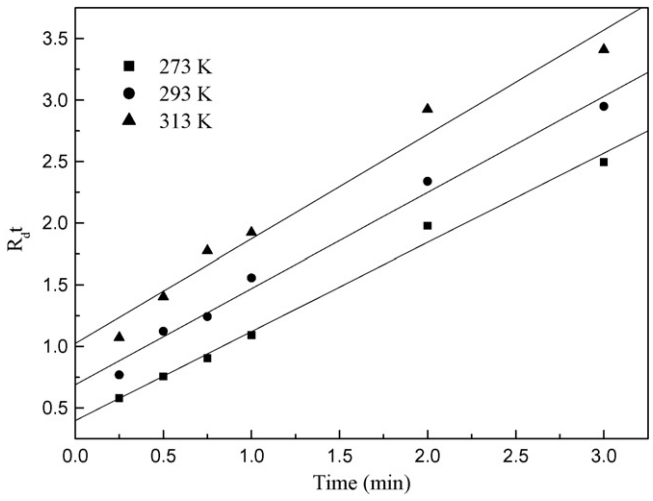

Fig. 4. Plots of *Rt* versus *t* for the adsorption of selenium ions on nano-TiO_2 at different temperatures.

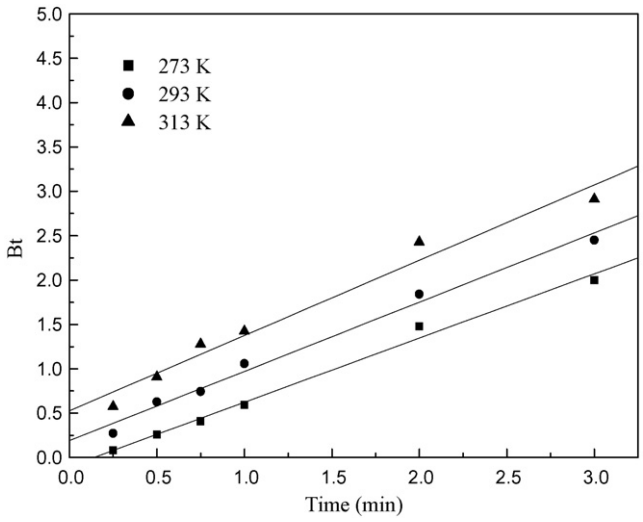

Fig. 5. Plots of *Bt* versus *t* for the adsorption of selenium ions on nano-TiO_2 at different temperatures.

result in Table 2. Arrhenius equation is as follows:

$$k = A\ \exp\left(\frac{-E_a}{RT}\right) \tag{4}$$

where A is the frequency factor (min^{-1}), E_a the activation energy ($kJ\,mol^{-1}$), R is the ideal gas constant ($J\,mol^{-1}\,K^{-1}$), T the absolute temperature (K).

Eq. (4) can be converted into Eq. (5) by taking logarithm

$$\ln k = \ln A - \frac{E_a}{RT} \tag{5}$$

Thus, E_a could be obtained from the slope of the line plotting $\ln k$ versus $1000/T$ and the estimated E_a for Se(IV) adsorption on nano-TiO_2 was 21.96 $kJ\,mol^{-1}$.

In order to ascertain the rate-controlling step, following equations of film and particle diffusion were applied to the adsorption kinetic data [16].

For film diffusion

$$R_d t = -\ln(1 - F) \tag{6}$$

For intraparticle diffusion

$$Bt = -\ln(1 - F) - 0.4977 \tag{7}$$

where $F = q_t/q_e$; q_t and q_e are the amounts of selenium ions adsorbed on nano-TiO_2 ($mg\,g^{-1}$) at time t (min) and at equilibrium time (min), respectively; R_d is the rate constant for film diffusion; $B = \pi^2 D_i/r^2$ (D_i is the inter-diffusion coefficient and r is the particle radius). Plots of $-\ln(1 - F)$ and *Bt* versus time, *t*, according to Eqs. (6) and (7), are shown in Figs. 4 and 5, respectively. Straight lines were obtained when $-\ln(1 - F)$ was plotted against *t* (Fig. 4) which did not pass through the origins. This indicates that film diffusion is not limiting step of the overall adsorption process kinetics. Fig. 5 indicates that straight lines were obtained on plotting *Bt* versus *t* which nearly passes through the origins. This shows that intraparticle diffusion may be the rate-controlling step [17].

Adsorption kinetic data was further processed to confirm whether intraparticle diffusion is the rate limiting and to find out the rate parameter for intraparticle diffusion. For such purpose Morris–Weber equation:

$$q_t = K_d t^{1/2} + I \tag{8}$$

The parameter K_d is the rate constant for intraparticle diffusion. Values of I give an idea about the thickness of the boundary layer, i.e., the larger the intercept, the greater is the boundary layer effect [18]. Plots of amount of selenium ions adsorbed against square roots of time, are shown in Fig. 6. This figure indicates that two distinct regions were observed, an initial linear portion which is due to the boundary layer diffusion effects and a second linear portion which is due to the intraparticle diffusion [17]. It was also observed that the lines do not pass through the origin, indicating that there is a boundary layer resistance and the magnitude of the intercepts are proportional to the extent of the boundary layer thickness. The change in the intercepts of the plots suggests that the mechanism of the adsorption of selenium ions on nano-TiO_2 is predominantly diffusion, and the intraparticle diffusion played a significant role in rate determining, but it was not the only main rate determining step through out the adsorption. Both intraparticle and boundary layer diffusion seem significant in the rate-controlling step. The intraparticle diffusion and boundary layer diffusion rates for selenium ions adsorption on nano-TiO_2 at different temperatures were calculated and their calculated values are given in Table 3.

3.6. Adsorption isotherm and adsorption capacity

The equilibrium adsorption amount of Se(IV) on nano-TiO_2 as a function of the equilibrium concentration of Se(IV) is shown in

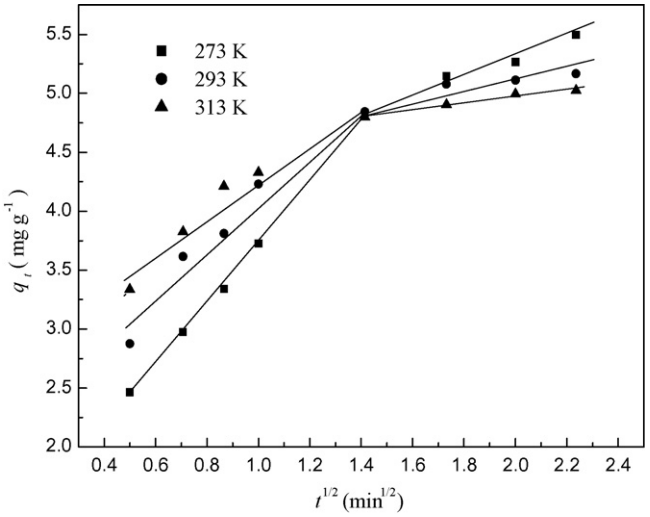

Fig. 6. Morris–Weber plots for kinetic modelling of Se(IV) adsorbed onto nano-TiO_2 at different temperatures.

Table 3
Calculated parameters for Se(IV) adsorption on nano-TiO_2 at different temperatures.

T (K)	Initial linear portion			Second linear portion		
	K_{d1} (mg g^{-1} min$^{-1/2}$)	I_1	r_1	K_{d2} (mg g^{-1} min$^{-1/2}$)	I_2	r_2
273	2.600	1.134	0.999	0.770	3.764	0.990
293	2.084	2.004	0.981	0.376	4.357	0.932
313	1.559	2.699	0.973	0.284	4.405	0.987

Data indicate that model parameters are statistically significant (t-test) at 95% confidence level.

Fig. 7. The adsorption for Se(IV) ions increased until the saturation was attained. Adsorption isotherm is important to describe how solutes interact with the sorbent.

The Langmuir model is often used to describe equilibrium sorption isotherms:

$$\frac{C_e}{q_e} = \frac{C_e}{q_m} + \frac{1}{bq_m} \quad (9)$$

where q_m is the maximum adsorption at monolayer (mg g^{-1}), C_e is the equilibrium concentration of Se(IV), q_e is the amount of Se(IV) adsorbed per unit weight of nano-TiO_2 at equilibrium concentration (mg g^{-1}) and b is the Langmuir constant related to the affinity of binding sites (L mg^{-1}).

The widely used empirical Freundlich equation based on sorption on a heterogeneous surface is given by:

$$\lg\ q_e = \lg K_F + \frac{1}{n}\lg C_e \quad (10)$$

where K_F and n are Freundlich constants indicating sorption capacity (mg g^{-1}) and intensity, respectively.

The Langmuir, Freundlich isotherm constants were determined from the plots of C_e/q_e against C_e, lg q_e versus lg C_e, respectively, at 273 K, 293 K and 313 K.

The isotherm constants for the isotherms studied, and the correlation coefficients with the experimental data are listed in Table 4. Langmuir and Freundlich isotherm model were statistically significant at a 95% confidence level. It is found that the adsorption of selenium on nano-TiO_2 were correlated well ($r > 0.99$) with the Langmuir equation as compared to the Freundlich equation ($r > 0.90$) under the concentration range studied. Therefore, Langmuir isotherm fitting is better than Freundlich isotherm in all conditions according to the correlation coefficients r. The maximum adsorption capacity of selenium ions on nano-TiO_2 is 8.46 mg g^{-1}, 7.71 mg g^{-1}, and 7.30 mg g^{-1} at 273 K, 293 K and 313 K, respectively.

The essential features of a Langmuir isotherm can be expressed in terms of a dimensionless constant separation factor or equilibrium parameter, R_L that is used to predict if an adsorption system is "favourable" or "unfavourable" [19]. The separation factor, R_L is defined by:

$$R_L = \frac{1}{1 + bC_0} \quad (11)$$

where C_0 is the initial Se(IV) concentration (mg mL^{-1}) and b is the Langmuir adsorption equilibrium constant (L mg^{-1}). Table 4 lists the calculated results. Based on the effect of separation factor on isotherm shape, the R_L values are in the range of 0–1, which indicates that the adsorption of Se(IV) on nano-TiO_2 are favourable.

The Dubinin–Radushkevich (D–R) [20] isotherm was also tested in its linearized form:

$$\ln\ q_e = \ln q_m - K\varepsilon^2 \quad (12)$$

where q_e and q_m have the same meaning as above, K is the parameter related to the adsorption energy. Polanyi defines the adsorption potential (ε) as the free energy change required moving a molecule from bulk solution to the adsorption space. The Polanyi potential varies with the solution concentration according to:

$$\varepsilon = RT\ \ln\left(1 + \frac{1}{C_e}\right) \quad (13)$$

where R is equal to ideal gas constant and T is the temperature (K). A straight line was obtained on plotting ln q_e versus ε^2 (shown in Fig. 8), indicating that Se(IV) adsorption also obeys the D–R equation. From the slope of the plot, a value of q_m (0.243 mmol g^{-1}, 293 K) has been evaluated for Se(IV). The adsorption energy for

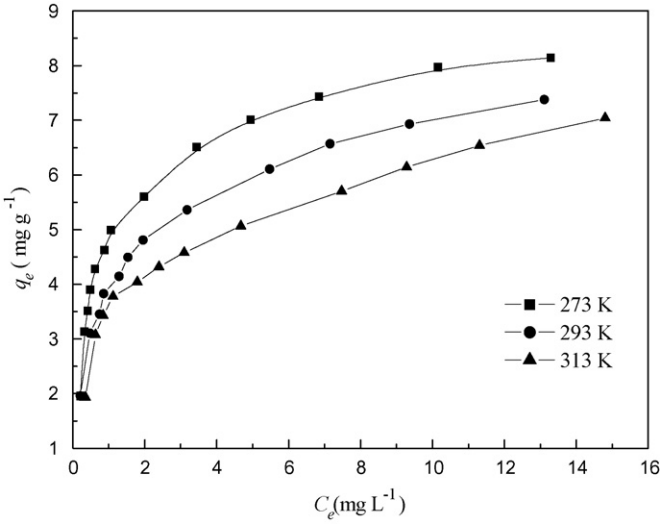

Fig. 7. Isotherm of Se (IV) adsorption on nano-TiO_2 at different temperatures (273 K, 293 K and 313 K); 50 mg of nano-TiO_2; the initial Se(IV) concentration range was 10.0–54.0 mg L^{-1}; pH 5.

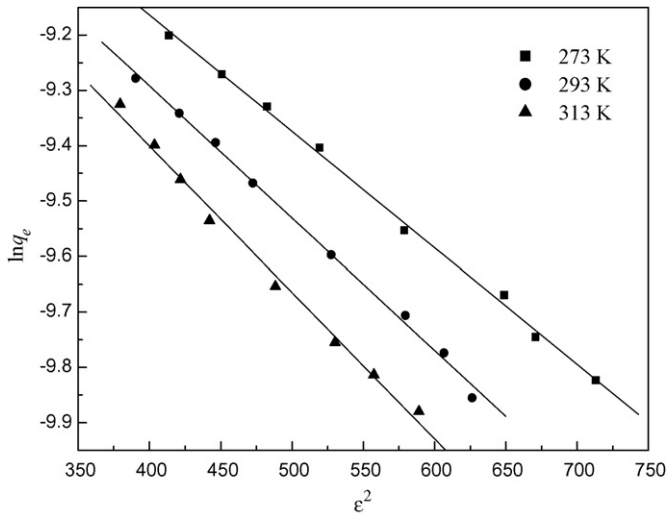

Fig. 8. D–R adsorption isotherm for Se(IV) adsorption on nano-TiO_2 at different temperatures (273 K, 293 K and 313 K); 50 mg of nano-TiO_2; the initial Se(IV) concentration range was 10.0–54.0 mg L^{-1}; pH 5.

Table 4
Langmuir Freundlich and D–R isotherm constants and correlation coefficients at the different temperatures.

T (K)	Langmuir				Freundlich			D–R		
	q_m (mg g^{-1})	b (L mg^{-1})	r	R_L	K_F (mg g^{-1})	n	r	q_m (mg g^{-1})	E (kJ mol^{-1})	r
273	8.46	1.36	0.999	0.013–0.068	4.37	3.48	0.978	19.19	15.43	0.999
293	7.71	0.98	0.998	0.020–0.093	3.72	3.38	0.983	18.87	14.46	0.998
313	7.30	0.72	0.995	0.027–0.123	3.24	3.24	0.954	18.79	13.74	0.996

Data indicate that model parameters are statistically significant (t-test) at 95% confidence level.

Se(IV) adsorption can be calculated by:

$$E = (-2K)^{-1/2} \quad (14)$$

The value of the adsorption energy was evaluated as 14.46 kJ mol^{-1}, indicating that the value lies within the energy range of ion-exchange reaction, i.e., 8–16 kJ mol^{-1} [21].

3.7. Thermodynamic studies

The experiments were carried out at 273 K, 293 K and 313 K for different concentrations The values of ΔH^0 were calculated from the slopes and intercepts of linear regression of ln C vesus $1/T$ using the Clausius–Clapeyron equation [22]:

$$\ln C = \frac{\Delta H}{RT} + D \quad (15)$$

where C is the equilibrium concentration of Se(IV) in solution (mg L^{-1}) at constant amount of sorbed Se(IV) and D is the intercept of the plot of ln C versus $1/T$. ΔH^0 was assumed to be constant for a constant surface coverage.

To calculate the values of the other parameters (ΔG^0, ΔS^0) the following equations were used:

$$K_C = \frac{C_{Be}}{C_{Ae}} \quad (16)$$

$$\Delta G^0 = -RT \ln K_C \quad (17)$$

$$\Delta S^0 = \frac{\Delta H^0 - \Delta G^0}{T} \quad (18)$$

where C_{Be} and C_{Ae} are the equilibrium concentrations of Se(IV) on the sorbent and solution, respectively, K_C is the equilibrium constant, ΔS^0 is standard entropy, ΔG^0 is standard free energy.

The values of ΔH^0, ΔS^0 and ΔG^0 were given in Table 5. The negative values of ΔH^0 and ΔG^0 show exothermic and spontaneous nature of sorption.

3.8. Sorption and recovery of selenium from water samples

The applicability of the proposed method for the quantitative collection and recovery of Se(IV) from natural water and industrial waste water samples. Good recoveries (95–105%) were reached for the analyzed samples. These data proved that the method is possible to achieve excellent accuracy.

Table 5
Thermodynamic parameters for the adsorption of Se(IV) on nano-TiO_2.

T (K)	273	290	313
K_c	7.08	4.59	3.31
ΔG^0 (kJ mol^{-1})	−4.44	−3.71	−3.12
ΔH^0 (kJ mol^{-1})	−11.20		
ΔS^0 (J mol^{-1} K^{-1})	−24.76	−25.56	−25.83

Data indicate that model parameters are statistically significant (t-test) at 95% confidence level.

3.9. Interference study

5 mL of 40 μg/mL selenium and 5 mL of each interfering ion solutions were added into a 50 mL Erlenmeyer flask. The concentration of foreign ions were chosen to be close or higher to their contents in natural waters. The influence of common anions and cations on the sorption was investigated. The results indicated that no interference were observed when Na^+ (100 mg), K^+ (80 mg), Ca^{2+} (4 mg), Mg^{2+} (4 mg), Mn^{2+} (5 mg), Ni^{2+} (5 mg), Co^{2+} (1 mg), Zn^{2+} (0.5 mg), Cr^{3+} (250 (g), ReO_4^- (4.5 mg), $Mo_7O_{24}^{6-}$ (0.1 mg), NO_3^- (400 mg), Cl^- (100 mg), Br^- (8 mg), SO_4^{2-} (25 mg), WO_4^{2-} (4 mg), SCN^- (4 mg) were added.

4. Conclusion

In this paper, the adsorption behavior of selenium on nano-TiO_2 was investigated. The main advantages of the procedure are ease and simple, and can rapidly attain phase equilibration. Besides, nano-TiO_2 as sorbents have high adsorption capacity. The experimental results indicate that nano-TiO_2 can effectively remove Se(IV) in aqueous solution in the range of pH 2–6. The percentage of Se(IV) removal by nano-TiO_2 is more than 96%. The kinetics of sorption follows a pseudo-second-order. The overall rate process appears to be influenced by both boundary layer diffusion and intraparticle diffusion. The adsorption isotherms could be well fitted by the Langmuir adsorption isotherm equations. The temperature variation has been used to evaluate the values of ΔH^0, ΔS^0 and ΔG^0. The negatives values of ΔH^0 and ΔG^0 show exothermic and spontaneous nature of sorption.

Acknowledgements

The authors greatly acknowledge Natural Science Foundation of Liaoning Province for financial support (nos. 2009R30 and 20082051). The authors also thank our colleagues and other students participating in this work.

References

[1] M. Rovira, J. Giménez, M. Martínez, X. Martínez-Lladó, Sorption of selenium(IV) and selenium(VI) onto natural iron oxides: goethite and hematite, J. Hazard. Mater. 150 (2008) 279–284.
[2] S. Lawson, J.M. Macy, Bioremediation of selenite in oil refinery wastewater, Appl. Microbiol. Biotechnol. 43 (4) (1995) 762–765.
[3] M. Kashiwa, S. Nishimoto, K. Takahashi, M. Ike, M. Fujita, Factors affecting soluble selenium removal by a selenate reducing bacterium *Bacillus* sp. SF-1, J. Biosci. Bioeng. 89 (6) (2000) 528–533.
[4] D. Peak, Adsorption mechanisms of selenium oxyanions at the aluminum oxide/water interface, J. Colloid Interface Sci. 303 (2006) 337–345.
[5] J. Das, D. Das, G.P. Dash, K.M. Parida, Studies on Mg/Fe hydrotalcite-like-compound (HTlc). I. Removal of inorganic selenite (SeO_3^{2-}) from aqueous medium, J. Colloid Interface Sci. 251 (1) (2002) 26–32.
[6] M. Duc, G. Lefèvre, M. Fédoroff, Sorption of selenite ions on hematite, J. Colloid Interface Sci. 298 (2) (2006) 556–563.
[7] A. Afkhami, Kinetic-spectrophotometric determination of selenium in natural water after preconcentration of elemental selenium on activated carbon, Talanta 58 (2002) 311–317.
[8] E.I. El-Shafey, Sorption of Cd(II) and Se(IV) from aqueous solution using modified rice husk, J. Hazard. Mater. 147 (2007) 546–555.
[9] E.I. El-Shafey, Removal of Se(IV) from aqueous solution using sulphuric acid-treated peanut shell, J. Environ. Manage. 84 (2007) 620–627.

[10] M. Martínez, J. Giménez, J. de Pablo, M. Rovira, L. Duro, Sorption of selenium (IV) and selenium (VI) onto magnetite, Appl. Surf. Sci. 252 (10) (2006) 3767–3773.
[11] Z.J. Gong, X.S. Zhang, G.H. Chen, Flow injection kinetic spectrophotometric determination of trace amounts of Se(IV) in seawater, Talanta 66 (2005) 1012–1017.
[12] S.D. Faust, O.M. Aly, Chemistry of Natural Waters, Ann Arbor Science, Ann Arbor, MI, 1981, pp. 359–371.
[13] T. Lin, Inorganic selenium speciation in groundwaters by solid phase extraction on Dowex 1X2, J. Hazard. Mater. 149 (2007) 80–85.
[14] Y. Liu, P. Liang, L. Guo, Nanometer titanium dioxide immobilized on silica gel as sorbent for preconcentration of metal ions prior to their determination by inductively coupled plasma atomic emission spectrometry, Talanta 68 (1) (2005) 25–30.
[15] S. Azizian, Kinetic models of sorption: a theoretical analysis, J. Colloid Interface Sci. 276 (1) (2004) 47–52.
[16] M.S. Shaukat, M.I. Sarwar, R. Qadeer, Adsorption of strontium ions from aqueous solution on Pakistani coal, J. Radioanal. Nucl. Chem. 265 (1) (2005) 73–79.
[17] R. Qadeer, Adsorption behavior of ruthenium ions on activated charcoal from nirtic acid medium, Colloids Surf. A 293 (2007) 217–223.
[18] V.S. Mane1, I.D. Mall, V.C. Srivastava, Kinetic and equilibrium isotherm studies for the adsorptive removal of Brilliant Green dye from aqueous solution by rice husk ash, J. Environ. Manage. 84 (4) (2007) 390–400.
[19] W.S. Wan Ngah, A. Kamari, Y.J. Koay, Equilibrium and kinetics studies of adsorption of copper(II) on chitosan and chitosan and chitosan/PVA beads, Int. J. Biol. Macromol. 34 (2004) 155–161.
[20] A. Kilislioglu, B. Bilgin, Thermodynamic and kinetic investigations of uranium adsorption on amberlite IR-118H resin, J. Appl. Radiat. Isotopes 58 (2) (2003) 155–160.
[21] S.Q. Memon, M.I. Bhanger, S.M. Hasany, Sorption behavior of impregnated Styrofoam for the removal of Cd(II) ions, Colloids Surf. A 279 (2006) 142–148.
[22] G. Bereket, A.Z. Aroguz, M.Z. Ozel, Removal of Pb(II), Cd(II), Cu(II) and Zn(II) from aqueous solutions by adsorption on bentonite, J. Colloid Interface Sci. 187 (2) (1997) 338–343.